

Alma Mater Studiorum Università di Bologna  
Archivio istituzionale della ricerca

Co-reactant-on-Demand ECL: Electrogenerated Chemiluminescence by the in Situ Production of S2O82- at Boron-Doped Diamond Electrodes

This is the final peer-reviewed author's accepted manuscript (postprint) of the following publication:

*Published Version:*

Irkham, Watanabe, T., Fiorani, A., Valenti, G., Paolucci, F., Einaga, Y. (2016). Co-reactant-on-Demand ECL: Electrogenerated Chemiluminescence by the in Situ Production of S2O82- at Boron-Doped Diamond Electrodes. JOURNAL OF THE AMERICAN CHEMICAL SOCIETY, 138(48), 15636-15641 [10.1021/jacs.6b09020].

*Availability:*

This version is available at: <https://hdl.handle.net/11585/591484> since: 2017-05-25

*Published:*

DOI: <http://doi.org/10.1021/jacs.6b09020>

*Terms of use:*

Some rights reserved. The terms and conditions for the reuse of this version of the manuscript are specified in the publishing policy. For all terms of use and more information see the publisher's website.

This item was downloaded from IRIS Università di Bologna (<https://cris.unibo.it/>).  
When citing, please refer to the published version.

(Article begins on next page)

This is the final peer-reviewed accepted manuscript of:

Irkham, T. Watanabe, A. Fiorani, G. Valenti, F. Paolucci, Y. Einaga.

Co-reactant-on-Demand ECL: Electrogenenerated Chemiluminescence by the in Situ Production of S<sub>2</sub>O<sub>8</sub><sup>2-</sup> at Boron-Doped Diamond Electrodes

J. Am. Chem. Soc. 2016, 138, 15636–15641

The final published version is available online at:  
<https://pubs.acs.org/doi/10.1021/jacs.6b09020>

#### Rights / License:

The terms and conditions for the reuse of this version of the manuscript are specified in the publishing policy. For all terms of use and more information see the publisher's website.

# Coreactant-on-Demand ECL: Electrogenenerated Chemiluminescence by the In-situ Production of $S_2O_8^{2-}$ at BDD Electrodes

Irkham,<sup>1</sup> Takeshi Watanabe,<sup>1</sup> Andrea Fiorani,<sup>2</sup> Giovanni Valenti,<sup>2</sup> Francesco Paolucci,<sup>2\*</sup> and Yasuaki Einaga<sup>1,3\*</sup>

<sup>1</sup> Department of Chemistry, Keio University, 3-14-1 Hiyoshi, Yokohama 223-8522, Japan

<sup>2</sup> Dipartimento di Chimica "Giacomo Ciamician", Università di Bologna, Via Selmi, 2, 40126, Bologna, Italy

<sup>3</sup> JST-ACCEL, 3-14-1 Hiyoshi, Yokohama 223-8522, Japan

KEYWORDS Boron Doped Diamond, Electrochemiluminescence, Coreactant, Sensor.

---

**ABSTRACT:** A novel *coreactant-free* electrogenerated chemiluminescence (ECL) system is developed where  $Ru(bpy)_3^{2+}$  emission is obtained on boron-doped diamond (BDD) electrodes. The method exploits the unique ability of BDD to operate at very high oxidation potential in aqueous solutions and to promote the conversion of inert  $SO_4^{2-}$  into the reactive coreactant  $S_2O_8^{2-}$ . This novel procedure is rather straightforward, not requiring any particular electrode geometry, and, since the coreactant is only generated in-situ the interference with biological samples is minimized. The underlying mechanism is similar to that of the  $Ru(bpy)_3^{2+}/S_2O_8^{2-}$  system; however the intensity of the emitted signal increases linearly with  $[SO_4^{2-}]$  up to  $\approx 0.6$  M, with possible implications for analytical uses of the proposed procedure.

---

## Introduction.

*Electrogenenerated Chemiluminescence* (ECL) is a redox-induced light emission in which species generated at electrodes undergo high-energy electron transfer reaction to form light emitting excited states.<sup>1-5</sup> The development of the so-called coreactant approach was a crucial point for the implementation of ECL as analytical technique since it permits to exploit the technique in environmentally-benign and user-friendly aqueous solutions. In fact the majority of commercially available ECL-based instrumentations employs this strategy.<sup>5-7</sup> According to the annihilation procedure, the excited state is generated by the reaction occurring at the electrode between radicals ensuing from the same species (i.e., the fluorophore).<sup>8</sup> Whereas, in coreactant ECL, the excited state is generated through the reaction between two different precursors, the fluorophore (often  $Ru(bpy)_3^{2+}$ , although alternative fluorophores are currently thoroughly investigated<sup>9-11</sup>) and the *coreactant*, whose electrochemical oxidation (or reduction) is first carried out. One of the most popular coreactant for  $Ru(bpy)_3^{2+}$  is tri-n-propylamine (TPA),<sup>12-17</sup> the  $Ru(bpy)_3^{2+}/TPA$  system being in fact at the basis of commercial ECL immunoassay and DNA analysis devices.<sup>15</sup>

Despite its great efficiency in generating ECL in biocompatible environments, TPA shows some disadvantages such as toxicity, high vapor pressure, and low solubility in aqueous solutions.<sup>2</sup> Relatively high coreactant concentrations are usually needed in order to obtain high emission and this may represent a severe drawback in some bioanalytical applications, where the existence of high concentrations of coreactant species can interfere with the target biochemical analyte.<sup>18</sup> Notice that, in some applications, the addition of TPA is not needed, since its role is played by the analyte itself, generally an amine, e.g., sarcosine,<sup>19</sup> dopamine,<sup>20</sup> NADH<sup>21</sup> or other organic compounds.<sup>22,23</sup> Furthermore, opportunely modified fluorophores may also limit the need for added TPA such as, e.g., in recently reported ruthenium(II) complexes carrying Schiff bases cavities. Due to the electrochemical oxidation of phenolic hydroxyl groups and the resonant structure of imino radicals, electrons are transferred intramolecularly to Ru(III) center leading to the efficient generation of the Ru(II)-based excited state.<sup>24</sup>

In order to maintain a more general analytical applicability, the *in-situ generation of coreactant* starting from a relatively unreactive precursor would however represent a promising alternative approach capable to keep the great advantages typical of such a highly sensitive technique. At the same time, it would allow to circumvent most of the aforementioned drawbacks such as toxicity issues and interferences with the biomolecules. In such a context, peroxydisulfate ( $S_2O_8^{2-}$ ) offers some advantages with respect to amines.  $S_2O_8^{2-}$  has widely been used as a coreactant in many ECL applications<sup>25-27</sup> where, upon cathodic reduction, it forms the sulfate radical anion ( $SO_4^{\cdot-}$ ), a strongly oxidizing intermediate.<sup>25,28</sup> It has been shown that the ECL efficiency for the  $Ru(bpy)_3^{2+}/S_2O_8^{2-}$  is about half that of the annihilation system.<sup>26</sup> Besides being coupled to common luminophores such as Ru complexes, luminol and their derivatives, peroxydisulfate was also shown to exhibit ECL behaviour at magnesium, silver and platinum electrodes, where dissolved oxygen can react with  $SO_4^{\cdot-}$ , thus generating

light-emitting species such as  $^1\text{O}_2$ ,  $^1(\text{O}_2)_2$  and  $^3(^1\text{O}_2)_2$ .<sup>29</sup> Several examples based on such an approach have recently been reported, such as a label-free and highly sensitive ECL aptasensor for kanamycin,<sup>30</sup> also coupled to nanocarbons,<sup>31</sup> quantum dots<sup>32</sup> and gold nanoclusters<sup>33,34</sup> for the high sensitive detection of chemicals,<sup>35</sup> antigens<sup>36</sup> and nucleic acids.<sup>37,38</sup> Importantly, peroxydisulfates are commercially prepared by the electrolytic oxidation of aqueous solutions of sulfate precursors, e.g., ammonium sulfate with platinum or platinized titanium anodes at high current densities. Therefore, the in-situ electrogeneration of peroxydisulfate represents a viable strategy to obtain a coreactant-free ECL system. In fact, the coreactant would be generated, at will and in-situ, by applying a suitably positive potential in a solution containing the sulfate precursor followed by the step to negative potential that can ignite the ECL emission. Notice that a similar procedure would not be accessible in the case of amines. Given the very high potential required to perform the anodic oxidation of sulfate to peroxydisulfate ( $E^\circ = 2.01 \text{ V vs. SHE}$ ), anode materials displaying very high overpotentials for the oxygen evolution reaction are however needed for the efficient production of peroxydisulfates. Boron-doped diamond (BDD) is known for its wider potential window compared to conventional electrodes, such as glassy carbon or metals (platinum, gold).<sup>39,40</sup> In particular, BDD has been proposed as anode to perform the efficient oxidization of  $\text{SO}_4^{2-}$  into peroxydisulfate<sup>41,42</sup> and it has been used for the development of laboratory devices for the determination of sulfates and peroxydisulfates, adapted for the on-line monitoring in process control applications.<sup>43</sup>

Moreover, in recent years, BDD has also been proposed as electrode material for ECL, in particular in applications using  $\text{Ru}(\text{bpy})_3^{2+}$  with either TPA<sup>16,17,44,45</sup> or alcohols and ethers<sup>39</sup> or finally with luminol.<sup>46</sup>

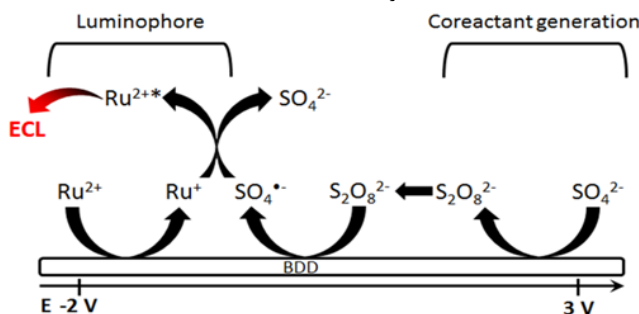


**Figure 1.** Reaction mechanism of electrochemiluminescence generation from  $\text{Ru}(\text{bpy})_3^{2+}$  on BDD electrode with sulfate ions. Ru =  $\text{Ru}(\text{bpy})_3$ .

Herein we report on a *coreactant-free ECL system* (Figure 1) in which the unique ability of BDD (i) to promote peroxydisulfate generation with high efficiency is coupled with (ii) the high overpotential for the hydrogen evolution reaction obtained at the same electrode to allow, in the end, the efficient ECL generation in a  $\text{Ru}(\text{bpy})_3^{2+}/\text{SO}_4^{2-}$  aqueous solution. The procedure is rather straightforward, not requiring any particular electrode geometry, and, since the reactive coreactant  $\text{S}_2\text{O}_8^{2-}$  is only generated on the electrode surface for a short time, the interference with biological samples is minimized.

## Experimental

**Materials.** All reagents were obtained commercially and used without further purification.  $\text{Ru}(\text{bpy})_3\text{Cl}_2 \cdot 6\text{H}_2\text{O}$ ,  $\text{Na}_2\text{SO}_4$ ,  $\text{Na}_2\text{S}_2\text{O}_8$ , and  $\text{KClO}_4$  were obtained from Sigma Aldrich. Pure water was doubly distilled with maximum conductivity  $18 \text{ M}\Omega$  obtained from Simply-Lab water system (DIRECT-Q 3 UV, Millipore).

**Preparation of BDD.** The BDD films were deposited on a silicon (111) wafer by using a microwave plasma-assisted chemical vapor deposition (MPCVD) system (CORNES Technologies / ASTeX-5400). Acetone and trimethoxyborane were used as the source of carbon and boron respectively with atomic ratio of B/C = 1%. The surface morphology of the BDD was examined with field emission scanning electron microscope (FESEM, JEOL JSM-7600F). Raman Spectra were recorded with an Acton SP2500 (Princeton Instruments) with excitation at  $532 \text{ nm}$  from a green laser diode in ambient temperature.

**Electrochemiluminescence measurement.** All ECL measurements were conducted in a conventional three electrode system in a PTFE cell with a 1% BDD, a platinum spiral, and an Ag/AgCl (Saturated KCl) as working, counter, and reference electrodes, respectively with PGSTAT302 (AUTOLAB Instrument).

The ECL signal was measured with a photomultiplier tube (PMT, Hamamatsu R4220p) placed in constant distance inside a dark box. A voltage  $750\text{--}800 \text{ V}$  was supplied to the PMT. The light/current/voltage curves were recorded by collecting the preamplified PMT output signal (by an ultralow-noise Acton research model 181) with the second input channel of the ADC module of the AUTOLAB instrument. For measuring the origin of the light, a voltage of  $800 \text{ V}$  was supplied to the PMT and the light measured directly without amplification. Stabilizing surface of the BDD electrode was carried out before each measurement by electrochemical cleaning by performing ten voltammetric cycles between  $-3.0 \text{ V}$  to  $3.0 \text{ V}$  followed by ten cycles between  $0 \text{ V}$  to  $-3.0 \text{ V}$  in  $0.1 \text{ M KClO}_4$  solution with scan rate  $0.3 \text{ V/s}$  (XPS characterization before and after the electrochemical treatment is reported in figure S1).

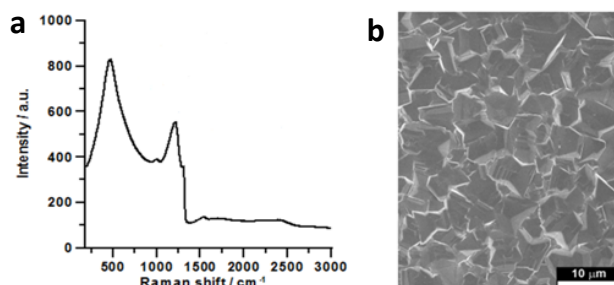


**Figure 2.** a) A Raman spectrum and b) a SEM image of 1% BDD.

#### Results and discussion.

The BDD used for the electrochemical and ECL measurements showed typical Raman spectrum for highly boron-doped diamond, exhibiting zone-center phonon line observed as a shoulder peak around  $1300\text{ cm}^{-1}$ . (Figure 2a).<sup>47</sup> SEM image of the BDD showed predominant facet having three-fold symmetry axis is (111) facet which is known as more electrochemically active domain than (100) (Figure 2b).<sup>44</sup>

The electrochemical and the ECL properties of  $\text{Ru}(\text{bpy})_3^{2+}$  in  $0.1\text{ M Na}_2\text{SO}_4$  aqueous solution on BDD electrodes were firstly investigated by cyclic voltammetry (CV). Figure 3 displays the CV curves (a) and the corresponding ECL-potential curves (b) obtained by scanning the potential initially from  $0\text{ V}$  to  $3.0\text{ V}$  followed by a scan to negative potentials ( $-2.0\text{ V}$ ).

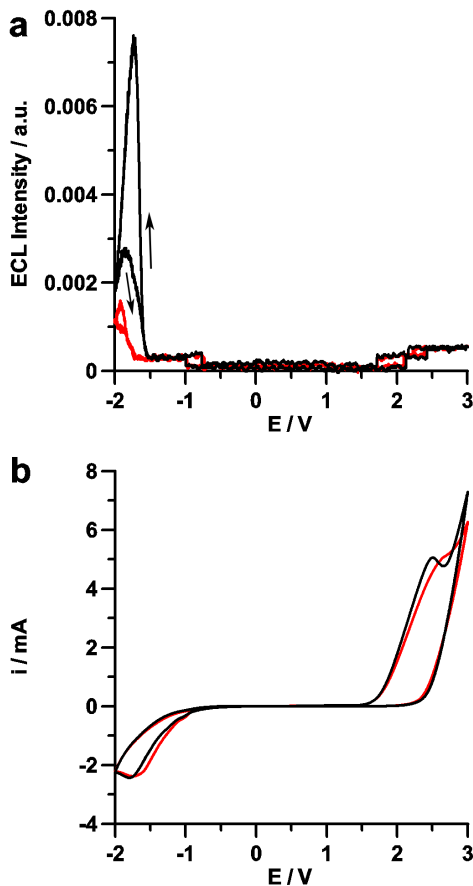


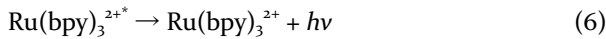
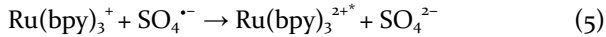
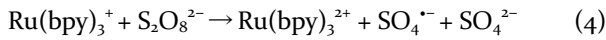
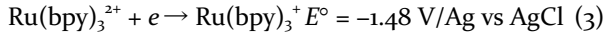
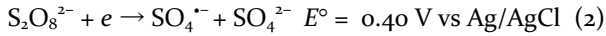
**Figure 3.** a) ECL and b) CV comparison between  $0.1\text{ M Na}_2\text{SO}_4$  (black) and  $0.1\text{ M KClO}_4$  (red) measurement of  $5\text{ }\mu\text{M Ru}(\text{bpy})_3\text{Cl}_2$  in water solvent. Scan rate  $100\text{ mV/s}$ , potential referred to  $\text{Ag/AgCl (KCl sat)}$  at room temperature. PMT bias  $750\text{ V}$ .

The first positive scan is meant to generate, at the BDD electrode surface, a sufficiently high concentration of peroxydisulfate ions (eq. 1) to fuel the ECL emission process during the negative potential scan, according to the following general mechanism

positive potential scan:

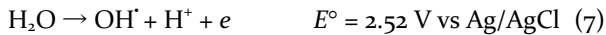


negative potential scan:

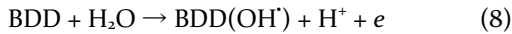


As shown in Figure 3a (black line), during the voltammetric cycle in 0.1 M aqueous  $\text{Na}_2\text{SO}_4$ , ECL was efficiently generated at  $E^\circ \leq -1.5 \text{ V}$ , i.e., in the region where reduction of both peroxydisulfate (reaction 2) and  $[\text{Ru}(\text{bpy})_3]^{2+}$  (reaction 3) may take place, thus making the sequence of processes outlined by equations 4-6 possible. Notice that, according to the established mechanism depicted above,<sup>26</sup> peroxydisulfate may be reduced to generate sulfate anion radical, either directly at the electrode (eq. 2) or by mediation of  $\text{Ru}(\text{bpy})_3^+$  (eq. 4). The profile of ECL emission vs. potential is similar to that obtained in the  $\text{Ru}(\text{bpy})_3^{2+}/\text{S}_2\text{O}_8^{2-}$  system (Figure S2), thus substantiating the above hypothesis that  $\text{S}_2\text{O}_8^{2-}$  coreactant is effectively produced at the BDD electrode during the first scan at positive potentials. In line with the above hypothesis, an intense ECL signal was only observed when potential was swept in the first scan to sufficiently high values, i.e., where the electrogeneration of peroxydisulfate occurs (Figure S3).

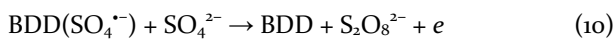
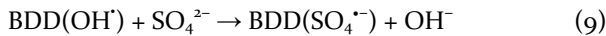
CV in 0.1 M aqueous  $\text{Na}_2\text{SO}_4$  (Figure 3b, black line) shows the broad and intense peak in the first scan at 2.5 V, indicating electrogeneration of peroxydisulfate. On the other hand, CV curve obtained in the absence of sulfate ions, i.e., in 0.1 M aqueous  $\text{KClO}_4$  (Figure 3b, red line) also shows comparable oxidation peak in similar potentials with somewhat duller shape. Such peak prior to intense oxygen evolution reaction (OER) is often observed at BDD electrodes. It is reported that this pre-OER peak is related to water oxidation reaction to generate hydroxyl radical (eq. 7) via surface redox couple of BDD.<sup>48</sup>



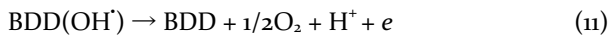
Hydroxyl radicals are considered to weakly interact with surface of BDD so that eq. 7 is formally written as:



where BDD represents the active site on the electrode surface. This reaction (8) may occur at slightly negative potential to  $E^\circ$  for equation (7) due to weak interaction to the surface of BDD. A. Kapalka et al. reported pre-OER peak attributed to eq. 8 was observed from 1.8 to 2.4 V vs. Ag/AgCl in 1 M  $\text{HClO}_4$  aqueous solution.<sup>48</sup> Furthermore, D. Khamis et al. reported that in the pre-OER potential domain, indirect oxidation process for generation of peroxydisulfate can occur via surface mediated reaction with  $\text{BDD}(\text{OH}^\cdot)$  as shown in following equations<sup>41</sup>



where the surface site  $\text{BDD}(\text{SO}_4^{\cdot-})$  is not as oxidative as  $\text{SO}_4^{\cdot-}$  but sufficient to lead to the generation of peroxydisulfate according to the overall mechanism depicted in eq. 1.<sup>41</sup> In the case of perchlorate solution, the oxidation current observed at pre-OER potential domain is considered as generation of oxygen (eq. 11) following reaction (8)<sup>48</sup>



In  $\text{Na}_2\text{SO}_4$  aqueous solutions, this reaction (11) also occurs at pre-OER potential domain as competing reaction with eq. 9. Actually, the CVs conducted in  $\text{N}_2$ -bubbled 0.1 M  $\text{Na}_2\text{SO}_4$  showed ORR peak in cathodic scan after sweeping until 2.5 V (Figure S4). Thus considering  $E^\circ$  value and similar oxidation current in pre-OER potential domain in both of  $\text{Na}_2\text{SO}_4$  and  $\text{KClO}_4$  solutions, water discharge reaction (eq. 8) is not fast and rate determining step around pre-OER potential domain i.e. around peak potential. Accordingly, in our experiment, it is considered that peroxydisulfate is mainly generated by indirect oxidation process thorough the reactions 8, 9 and 10.

In cathodic scan, large reduction peak observed starting around  $-1.0 \text{ V}$  in both solutions of  $\text{Na}_2\text{SO}_4$  and  $\text{KClO}_4$  is mainly due to oxygen reduction reaction (ORR) since oxygen can be produced in first positive scan (see Figure S4). The reductions of

both peroxydisulfate (reaction 2) and  $[\text{Ru}(\text{bpy})_3]^{2+}$  (reaction 3) were considered to be masked with this ORR peak. Despite occurrence of ORR, massive hydrogen evolution reaction (HER) that would more greatly inhibit the process leading to ECL at very negative potentials, could be avoided because of choosing  $\text{Na}_2\text{SO}_4$  instead of  $\text{H}_2\text{SO}_4$  or  $\text{NaHSO}_4$ , as precursor of electrogenerated peroxydisulfate.

Furthermore, BDD was uniquely suited to promote ECL emission under such conditions, since parallel experiments carried out with either Pt or glassy carbon electrodes were unsuccessful (Figure S5); at such electrodes, water oxidation proceeds via different route and even if hydroxyl radicals can be produced, the radicals would react with electrodes themselves rather than the sulfate ions.

Importantly, the ECL spectrum (Figure 4), recorded during chronoamperometric experiments (v. infra), shows a maximum wavelength at 609 nm, which is expectedly in full agreement with the attribution of the emitted light to the  $\text{Ru}(\text{bpy})_3^{2+}$  based excited state and excluding that other potential emitters, such as oxygen, may be playing an important role in the observed phenomenon.<sup>26</sup>

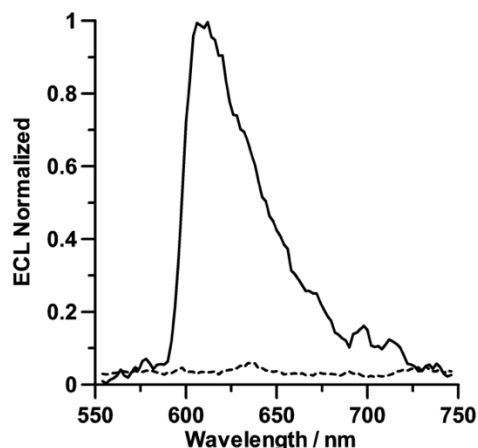
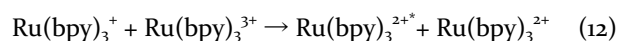


**Figure 4.** Normalized ECL spectrum of 5  $\mu\text{M}$   $\text{Ru}(\text{bpy})_3\text{Cl}_2$  / 0.1 M  $\text{Na}_2\text{SO}_4$  system (solid line) and 5  $\mu\text{M}$   $\text{Ru}(\text{bpy})_3\text{Cl}_2$  / 0.1 M  $\text{KClO}_4$  system (dashed line) in aqueous solution. PMT bias 800 V.

Interestingly, a weak emission was also obtained when potential was swept in the first scan up to 1.5 V, i.e., at potentials too low to produce peroxydisulfate, but sufficiently high to oxidise the  $\text{Ru}(\text{bpy})_3^{2+}$  fluorophore ( $E^\circ = 1.02$  V vs Ag/AgCl, see Figure S3, inset). A possible explanation for such a weak emission is therefore that, in the present system, ECL generation may also take place according to the annihilation route (eq. 12), where  $\text{Ru}(\text{bpy})_3^{3+}$  generated in the first (positive) scan may react with  $\text{Ru}(\text{bpy})_3^+$  generated in the second (negative) one:<sup>49</sup>



Such a mechanism, that involves the couple of fluorophores in either their oxidized or reduced form, is generally unobserved in aqueous media where the prevailing HER prevents formation of the reduced species  $\text{Ru}(\text{bpy})_3^+$ <sup>26</sup> while it would be made possible in the present case by the high overpotential for HER on BDD. In line with such a hypothesis, Figure 3a (red line) shows the ECL-potential plot obtained in 0.1 M  $\text{KClO}_4$  solutions, i.e., in the absence of sulfate ions, displaying a noticeable, although very weak signal, associated to process (12). Notice that annihilation ECL for aqueous  $\text{Ru}(\text{bpy})_3^{2+}$  solutions was only previously reported in the case of interdigitated carbon microelectrode arrays, with 2  $\mu\text{m}$  width spacing, working in a generation/collection biasing mode.<sup>50</sup> In the present case, instead, annihilation ECL would be obtained from  $\text{Ru}(\text{bpy})_3^{2+}$  aqueous solutions only by virtue of the unique properties of BDD electrodes, without requiring any particular geometry of the cell and electrodes system.

Further insight in the underlying mechanism - and quantification - of the ECL emission in the present system, was obtained by performing chronoamperometric experiments where potential was firstly stepped from 0 V to 3.0 V, where it was kept for various time durations ( $t_{\text{ox}}$ ) to generate variable amounts of coreactant, and then to -2.0 V to ignite the ECL process (see Figure 5b, inset); the current (Figure S6) and ECL light (Figure 5b) signals were continuously monitored. While the current curves decrease monotonically, the ECL signal exhibits a steep increase, after each complete oxidation-reduction cycle, followed by a rapid decay, reflecting the complex sequence of processes described by Eqs. 1-6 involving the production and encounter of the reacting species in the diffusion layer. Oxidation currents measured in the first step, in either the presence or absence of sulfate ions, were integrated and were found to increase linearly with the oxidation time  $t_{\text{ox}}$  (Figure 5a), thus suggesting that formation of the surface reactive species (eq. 8), rather than diffusion of the sulfate precursor, controls in the present conditions the oxidation current. By contrast, the integrated ECL signals (measured during the step at -2.0 V) decreases linearly with the square root of  $t_{\text{ox}}$  (Figure 5b, inset) indicating that the efficiency of the overall ECL

generation process is limited by diffusion of sulfate precursor to the electrode and of electrogenerated peroxydisulfate towards the bulk of solution.

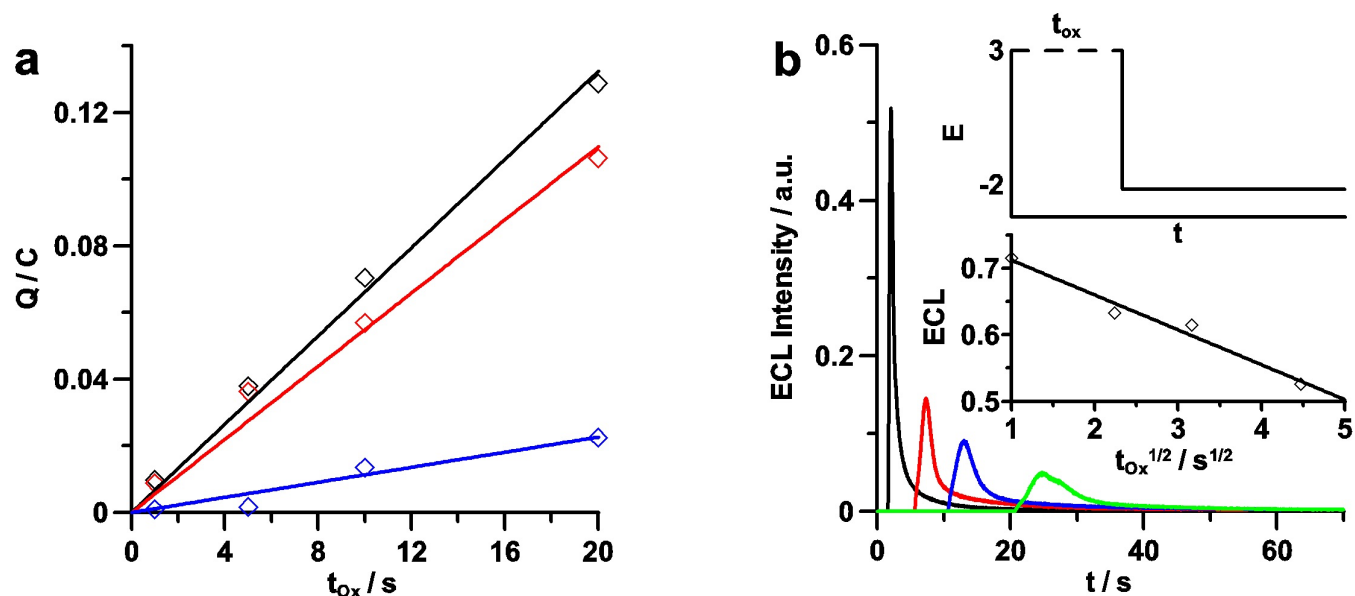


**Figure 5.** a) Integrated charge at 3.0 V for different oxidation times for 0.1 M  $Na_2SO_4$  (black), 0.1 M  $KClO_4$  (red) and the differences (blue) and b) ECL intensity transients measured during chronoamperometric experiments carried out in a 5  $\mu M$   $Ru(bpy)_3Cl_2$  and 0.1 M  $Na_2SO_4$  aqueous solution; first step from 0 to 3.0 V for  $t_{ox} = 1, 5, 10$  or 20 s, followed by a step to -2.0 V for 50 s. The ECL transients are displaced along the timescale according to the increasing of the oxidation step duration ( $t_{ox}$ ). Figure b inset: (above) potential program used in the chronoamperometric experiments; (below) integrated ECL intensity vs square root of time step duration  $t_{ox}$ . PMT bias 750

The efficiency of ECL generation was finally investigated at various sulfate concentrations. Current efficiency for sulfuric acid oxidation to peroxydisulfuric acid has been reported to increase with  $\text{H}_2\text{SO}_4$  concentration.<sup>51</sup> In the present case, the efficiency of peroxydisulfate electrogeneration was in fact found to increase linearly with  $[\text{SO}_4^{2-}]$  up to  $\approx 0.6$  M, then deviating negatively at higher concentrations (Figure S7), i.e., at significantly lower concentration than the reported maximum current efficiency for peroxydisulfate electrogeneration, obtained with sulfuric acid concentration  $\geq 2$  M.<sup>51</sup> Importantly, deviations from linearity of the ECL signal as a function of sulfate concentration (in the range  $10^{-3}$ –1 M, Figure 6), occurred at significantly lower values than those observed for current, since the signal, following an initial linear increase (up to 0.1 M), reaches a plateau at  $[\text{SO}_4^{2-}] \approx 0.5$  M. A similar trend was also observed in the ECL efficiency (i.e., after normalization by the  $\text{S}_2\text{O}_8^{2-}$  amount, see figure S8).

The observed trend of ECL intensity vs. sulfate precursor concentration can tentatively be ascribed to the known ability of peroxydisulfate ion to effectively quench the excited state  $\text{Ru}(\text{bpy})_3^{2+*}$ .<sup>26</sup> It has been reported that the ECL intensity of the  $\text{Ru}(\text{bpy})_3^{2+}/\text{S}_2\text{O}_8^{2-}$  system is in fact a function of  $\text{S}_2\text{O}_8^{2-}$  concentration with a maximum emission at  $[\text{S}_2\text{O}_8^{2-}] \approx 15$ –20 mM.<sup>26</sup> The dependence of the ECL intensity vs.  $[\text{SO}_4^{2-}]$  observed in the present case would therefore reflect the increasing competition, as the sulfate ions concentration increases, between the two processes associated to the electrogenerated peroxydisulfate, one leading to a more efficient ECL production (through an increased rate of peroxydisulfate generation) and the other to a faster quenching of the excited state.<sup>52,53</sup>

Finally, analytical applications of the present system can be envisaged within the observed linearity range (1–100 mM). BDD electrodes were proposed for the detection and measurement of sulfate ions, with detection limits in the grams per liter range ( $\approx 10$  mM), through their anodic oxidation to peroxydisulfate followed by the amperometric detection of peroxydisulfate (eq. 2), and some commercial development has been proposed.<sup>43,54</sup> In such a context, the present ECL-based approach would therefore allow to reach detection limits for sulfate ions in the millimolar range, i.e., at least one order of magnitude lower than the reported amperometric method.

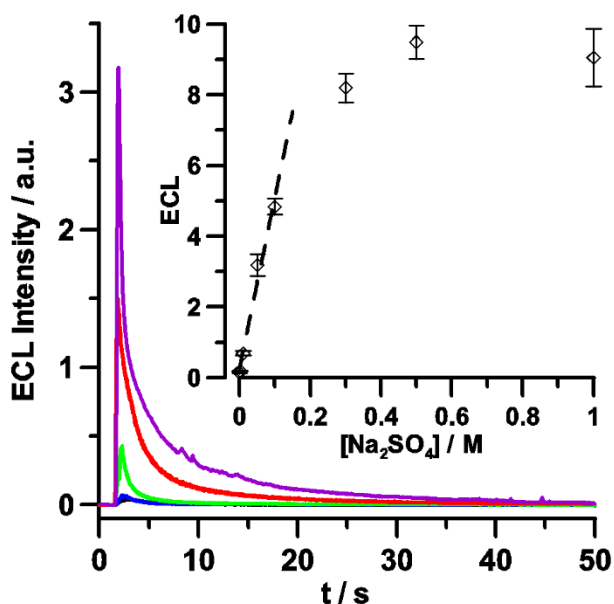


**Figure 6.** ECL intensity transient at various  $\text{Na}_2\text{SO}_4$  concentrations in 5  $\mu\text{M}$   $\text{Ru}(\text{bpy})_3\text{Cl}_2$  aqueous solutions; first step 3.0 V for 1 s, followed by a step to  $-2.0$  V for 50 s.  $\text{Na}_2\text{SO}_4$ : 1 mM (blue), 10 mM (green), 0.1 M (red), 1 M (purple) and 0.1 M  $\text{KClO}_4$  (black), Inset: integrated ECL intensity as function of concentration. PMT bias 750 V.

## Conclusions.

The generation of ECL from aqueous solutions containing the  $\text{Ru}(\text{bpy})_3^{2+}$  fluorophore and  $\text{SO}_4^{2-}$  was for the first time reported. The underlying mechanism is similar to that of the  $\text{Ru}(\text{bpy})_3^{2+}/\text{S}_2\text{O}_8^{2-}$  system, except that  $\text{S}_2\text{O}_8^{2-}$  is in this case electrogenerated in situ from the sulfate precursor, exploiting the unique ability of BDD electrodes to promote electrochemical reactions with compounds that have highly positive standard potentials. The intensity of the emitted signal was found to increase linearly with  $[\text{SO}_4^{2-}]$  up to  $\approx 0.6$  M, thus opening possible analytical uses of the present

approach with detection limits for sulfate ions as low as 1 mM. Finally, evidence was also found of ECL emission generated by Ru(bpy)<sub>3</sub><sup>2+</sup> through the annihilation mechanism, an unprecedented result in aqueous solutions that would also be associated to the wide potential windows achievable with BDD.

## ASSOCIATED CONTENT

### Supporting Information

ECL emission in acetonitrile, cyclic voltammetry in deaerated solution, effect of different electrode materials, effect of oxidation time, integrated anodic charge as a function of Na<sub>2</sub>SO<sub>4</sub> concentration [Fig. S1-S8]. The Supporting Information is available free of charge on the ACS Publications website.

## AUTHOR INFORMATION

### Corresponding Author

\*Y.E. einaga@chem.keio.ac.jp; F.P. Francesco.paolucci@unibo.it.

## ACKNOWLEDGMENT

We thank the University of Bologna, Italian Ministero dell'Istruzione, Università e Ricerca (MIUR-project PRIN 2010) and FARB, Fondazione Cassa di Risparmio in Bologna.

## ABBREVIATIONS

BDD Boron Doped Diamond.

ECL Electrogenerated Chemiluminescence

## REFERENCES

- (1) *Electrogenerated Chemiluminescence*; Bard, A. J., Ed.; Marcel Dekker: New York, 2004.
- (2) Richter, M. M. *Chem. Rev.* **2004**, *104*, 3003.
- (3) Forster, R. J.; Bertonecello, P., & Keyes, T. E. *Annu. Rev. Anal. Chem.* **2009**, *2*, 359.
- (4) Hu, L.; Xu, G. *Chem. Soc. Rev.* **2010**, *39* (8), 3275.
- (5) Hesari, M.; Ding, Z. *J. Electrochem. Soc.* **2016**, *163* (4), H3116.
- (6) Miao, W. **2008**, 2506.
- (7) Liu, Z.; Qi, W.; Xu, G. *Chem. Soc. Rev.* **2015**, *44* (10), 3117.
- (8) Valenti, G.; Fiorani, A.; Motta, S. Di; Bergamini, G.; Gingras, M.; Ceroni, P.; Negri, F.; Paolucci, F.; Marcaccio, M. *Chem. - A Eur. J.* **2015**, *21* (7), 2936.
- (9) Kerr, E.; Doeven, E. H.; Barbante, G. J.; Hogan, C. F.; Hayne, D. J.; Donnelly, P. S.; Francis, P. S. *Chem. Sci.* **2016**, *7*, 5271.
- (10) Zhou, Y.; Gao, H.; Wang, X.; Qi, H. *Inorg. Chem.* **2015**, *54* (4), 1446.
- (11) Della Ciana, L.; Zanarini, S.; Perciaccante, R.; Marzocchi, E.; Valenti, G. *J. Phys. Chem. C* **2010**, *114* (8), 3653.
- (12) Deaver, D. R. *Nature*. 1995, pp 758–760.
- (13) Leland, J. K. *J. Electrochem. Soc.* **1990**, *137* (10), 3127.
- (14) Noffsinger, J. B.; Danielson, N. D. *Anal. Chem.* **1987**, *59*, 865.
- (15) Miao, W.; Choi, J. P.; Bard, A. J. *J. Am. Chem. Soc.* **2002**, *124* (48), 14478.
- (16) Yang, Y.; Oh, J. W.; Kim, Y. R.; Terashima, C.; Fujishima, a; Kim, J. S.; Kim, H. *Chem. Commun.* **2010**, 46 (31), 5793.
- (17) Honda, K.; Yoshimura, M.; Rao, T. N.; Fujishima, a. *J. Phys. Chem. B* **2003**, *107* (7), 1653.
- (18) Xu, J.; Huang, P.; Qin, Y.; Jiang, D.; Chen, H. *Anal. Chem.* **2016**, *88* (9), 4609.
- (19) Valenti, G.; Rampazzo, E.; Biavardi, E.; Villani, E.; Fracasso, G.; Marcaccio, M.; Bertani, F.; Ramarli, D.; Dalcanale, E.; Paolucci, F.; Prodi, L. *Faraday Discuss.* **2015**, *185*, 1.
- (20) Stewart, A. J.; Hendry, J.; Dennany, L. *Anal. Chem.* **2015**, *87* (23), 11847.
- (21) De Poulpiquet, A.; Diez-Buitrago, B.; Dumont Milutinovic, M.; Sentic, M.; Arbault, S.; Bouffier, L.;

This item was downloaded from IRIS Università di Bologna (<https://cris.unibo.it/>)

**When citing, please refer to the published version.**

- Kuhn, A.; Sojic, N. *Anal. Chem.* **2016**, acs.analchem.6b01434.
- (22) Yuan, Y.; Han, S.; Hu, L.; Parveen, S.; Xu, G. *Electrochim. Acta* **2012**, 82, 484.
  - (23) Kebede, N.; Francis, P. S.; Barbante, G. J.; Hogan, C. F. *Analyst* **2015**, 140 (21), 7142.
  - (24) Li, P.; Jin, Z.; Zhao, M.; Xu, Y.; Guo, Y.; Xiao, D. *Dalton Trans.* **2015**, 44 (5), 2208.
  - (25) Bolleta, F.; Ciano, M.; Balzani, V.; Serpone, N. *Inorganica Chim. Acta* **1982**, 62 (C), 207.
  - (26) White, H. S.; Bard, A. J. *J. Am. Chem. Soc.* **1982**, 104 (25), 6891.
  - (27) Ege, D.; Becker, W. G.; Bard, A. J. *Anal. Chem.* **1984**, 56 (13), 2413.
  - (28) Memming, R.; Soc, J. E.; Memming, R. **1969**, 116 (6), 785.
  - (29) Reshetnyak, O. V.; Koval, E. P. *Electrochem. commun.* **1998**, 43 (839304), 465.
  - (30) Zhao, M.; Zhuo, Y.; Chai, Y. Q.; Yuan, R. *Biomaterials* **2015**, 52 (1), 476.
  - (31) Wu, L.; Wang, J.; Ren, J.; Li, W.; Qu, X. *Chem. Commun. (Camb)*. **2013**, 49 (50), 5675.
  - (32) Liang, J.; Yang, S.; Luo, S.; Liu, C.; Tang, Y. *Microchim. Acta* **2014**, 181 (7–8), 759.
  - (33) Hesari, M.; Workentin, M. S.; Ding, Z. *ACS Nano* **2014**, 8 (8), 8543.
  - (34) Wang, T.; Wang, D.; Padelford, J. W.; Jiang, J.; Wang, G. J. *Am. Chem. Soc.* **2016**, 138 (20), 6380.
  - (35) Yuan, D.; Chen, S.; Yuan, R.; Zhang, J.; Zhang, W. *Analyst* **2013**, 138 (20), 6001.
  - (36) Zhang, F.; Mao, L.; Zhu, M. *Microchim. Acta* **2014**, 181 (11–12), 1285.
  - (37) Cheng, Y.; Lei, J.; Chen, Y.; Ju, H. *Biosens. Bioelectron.* **2014**, 51, 431.
  - (38) Sun, H.; Ma, S.; Li, Y.; Qi, H.; Ning, X.; Zheng, J. *Biosens. Bioelectron.* **2016**, 79, 92.
  - (39) Honda, K.; Yamaguchi, Y.; Yamanaka, Y.; Yoshimatsu, M.; Fukuda, Y.; Fujishima, A. *Electrochim. Acta* **2005**, 51, 588.
  - (40) Yamanaka, Y.; Miyamoto, M.; Tanaka, Y.; Nagumo, a.; Katsuki, Y.; Fukuda, Y.; Yoshimatsu, M.; Takeshige, a.; Kondo, T.; Fujishima, a.; Honda, K. *Electrochim. Acta* **2008**, 53 (16), 5397.
  - (41) Khamis, D.; Mahé, E.; Dardoize, F.; Devilliers, D. *J. Appl. Electrochem.* **2010**, 40 (10), 1829.
  - (42) Hippauf, F.; Dorfler, S.; Zedlitz, R.; Vater, A.; Kaskel, S. *Electrochim. Acta* **2014**, 147, 589.
  - (43) Provent, C.; Haenni, W.; Santoli, E.; Rychen, P. *Electrochim. Acta* **2004**, 49, 3737.
  - (44) Honda, K.; Noda, T.; Yoshimura, M.; Nakagawa, K.; Fujishima, A. *J. Phys. Chem. B* **2004**, 108, 16117.
  - (45) Sentic, M.; Virgilio, F.; Zanut, A.; Manojlovic, D.; Arbault, S.; Tormen, M.; Sojic, N.; Ugo, P. *Anal. Bioanal. Chem.* **2016**, 408 (25), 7085.
  - (46) Garcia-Segura, S.; Centellas, F.; Brillas, E. J. *J. Phys. Chem. C* **2012**, 116 (29), 15500.
  - (47) Watanabe, T.; Honda, Y.; Kanda, K.; Einaga, Y. *Phys. Status Solidi Appl. Mater. Sci.* **2014**, 211 (12), 2709.
  - (48) Kapalka, A.; Fóti, G.; Comninellis, C. *Electrochim. Acta* **2007**, 53 (4), 1954.
  - (49) Tokel, N. E.; Bard, A. J. *J. Am. Chem. Soc.* **1972**, 94 (8), 2862.
  - (50) Fiaccabrino, G. C.; Koudelka-Hep, M.; Hsueh, Y. T.; Collins, S. D.; Smith, R. L. *Anal. Chem.* **1998**, 70 (19), 4157.
  - (51) Serrano, K.; Michaud, P. a.; Comninellis, C.; Savall, a. *Electrochim. Acta* **2002**, 48 (4), 431.
  - (52) White, H. S.; Becker, W. G.; Bard, A. J. *J. Phys. Chem.* **1984**, 88 (9), 1840.
  - (53) Lewandowska-Andralojc, a.; Polyansky, D. E. *J. Phys. Chem. A* **2013**, 117 (40), 10311.
  - (54) <http://www.neocoat.ch> (accessed June 28, 2016).